Supporting Information

Residual Dipolar Couplings as a Tool for Structural Analysis of Ionic Liquids

Higor D. F. de Melo,[a] Daiane S. Carvalho,[a] Fernando Hallwass,[a] Ulrich Sternberg[b,c] and Armando Navarro-Vázquez*[,a]

[a]Departamento de Química Fundamental, Centro de Ciências Exatas e da Natureza (CCEN), Universidade Federal de Pernambuco, Avenida Jornalista Fernandes s/n. Cidade Universitária. 50740-560, Recife, Pernambuco, Brazil.

[b]Research Partner of Karlsruhe Institue of Technology (KIT), Karslruhe Germany.

[c]COSMOS-Software, Jena, Germany. http://www.cosmos-software.de.

1. Description of NMR experiments

All NMR experiments, for the IL swollen gels in the relaxed and compressed states, were performed on an Agilent 400 MHz spectrometer, operating at 298 K, with resonance frequencies of 399.75 MHz for 1H, 61.36 MHz for 2H, and 100.52 MHz for 13C.

The ^{1}H NMR spectrum was acquired using a single pulse sequence, with a 45º pulse of 5.35 μs, acquisition time of 2.55 s, 8 transients, relaxation delay of 1.0 s, spectral width of 6400 Hz.

The ^{13}C NMR spectrum was acquired with a 45º pulse of 4.86 μs, acquisition time of 1.31 s, relaxation delay of 1.0 s, spectral width of 25.0 kHz, 80 transients for BMIM·NTf_2^- in DMA/ACN gel (75:25 v/v), 128 transients for EMIM·BF_4^- and BMIM·$[N(CN)_2]^-$ in DMA/ACN gel (75:25 v/v).

The gated-decoupled $\{^{1}H\}$-^{13}C spectra were acquired with an acquisition time of 1.31 s, relaxation delay of 1.0 s, spectral width of 25.0 kHz, 80 transients for BMIM·NTf_2^- in DMA/ACN gel (75:25 v/v), 256 transients for EMIM·BF_4^- and BMIM·$[N(CN)_2]^-$ in DMA/ACN gel (75:25 v/v).

The one-dimensional 1D-NOESY spectrum was performed using the Agilent provided DPFGSE[1] experiment with acquisition time of 2.55 s, 64 transients, relaxation delay of 1.0 s and spectral width of 4.0 kHz, the mixing time was 300 ms for BMIM·NTf_2^- in DMA/ACN gel (75:25 v/v), and 500 ms for EMIM.BF_4^- in DMA/ACN gel (75:25 v/v) and 500 ms for BMIN·$[(CN)_2N]^-$.

All NMR experiments were run unlocked.

2. NMR spectra of Ionic Liquid BMIM·NTf_2^-

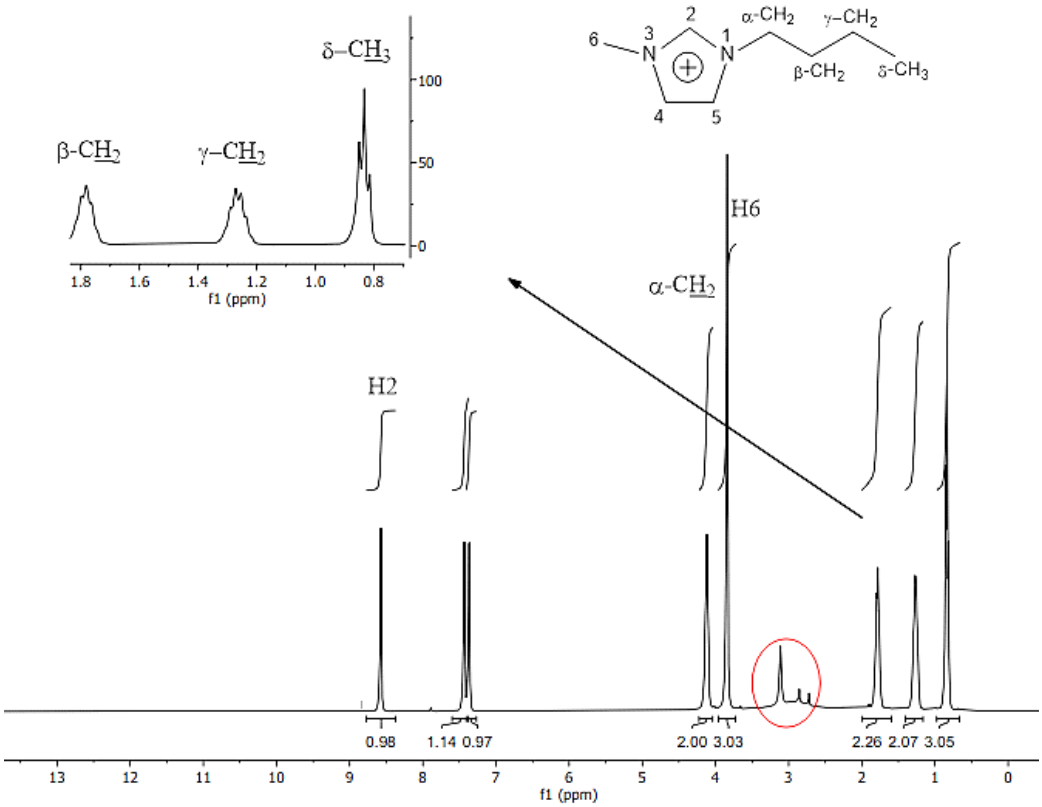

Figure S1. ^{1}H NMR spectrum (399.75 MHz) of compound BMIM·NTf_2^- on DMA/ACN gel (75:25 v/v) in relaxed state at 298K.

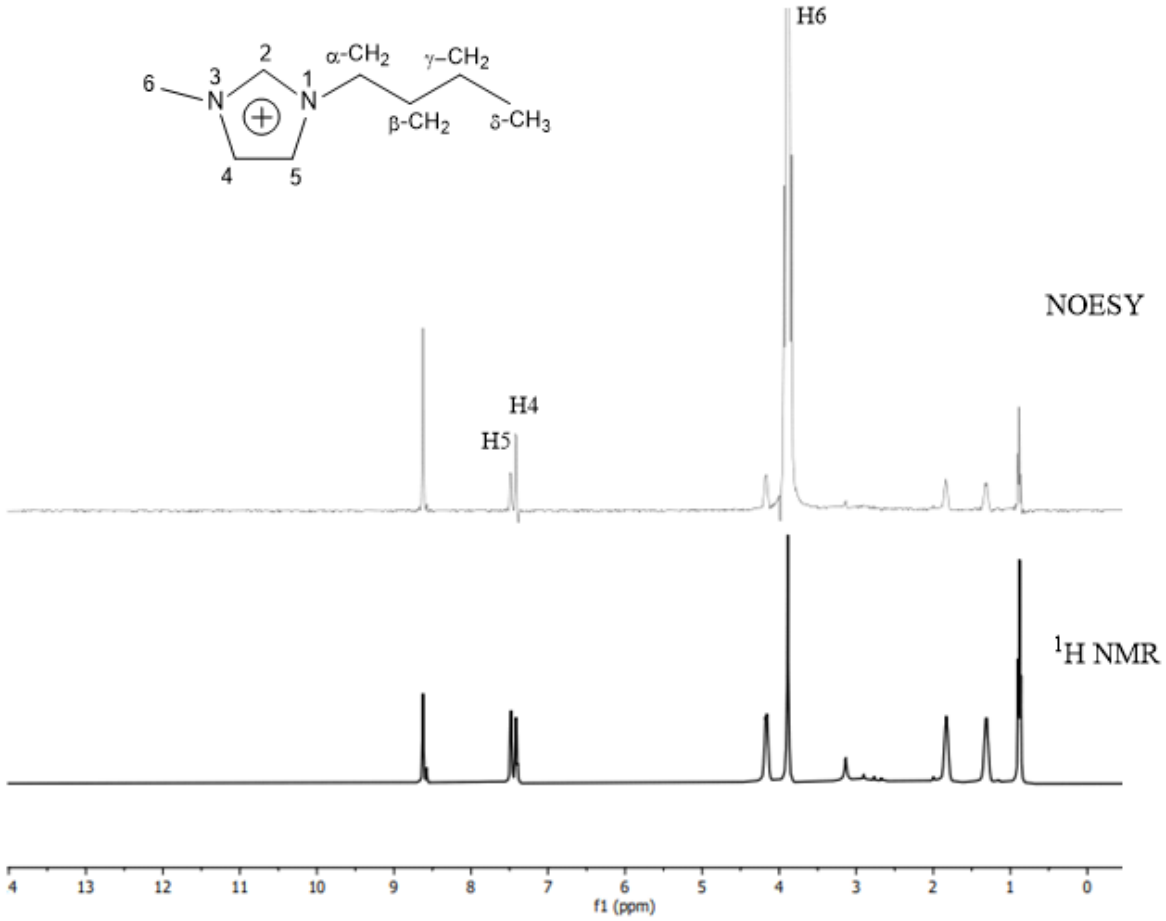

Figure S2. Top: 1D-NOESY (mixing time: 300 ms) (top) and standard ^{1}H (bottom) spectra of [BMIM·NTf_2^-] in the DMA/ACN gel (75:25 v/v) in the relaxed state at 298K. The Me6 signal for the IL inside the gel was selectively inverted. Note the negative NOE effects observed in the 1D-NOESY spectrum.

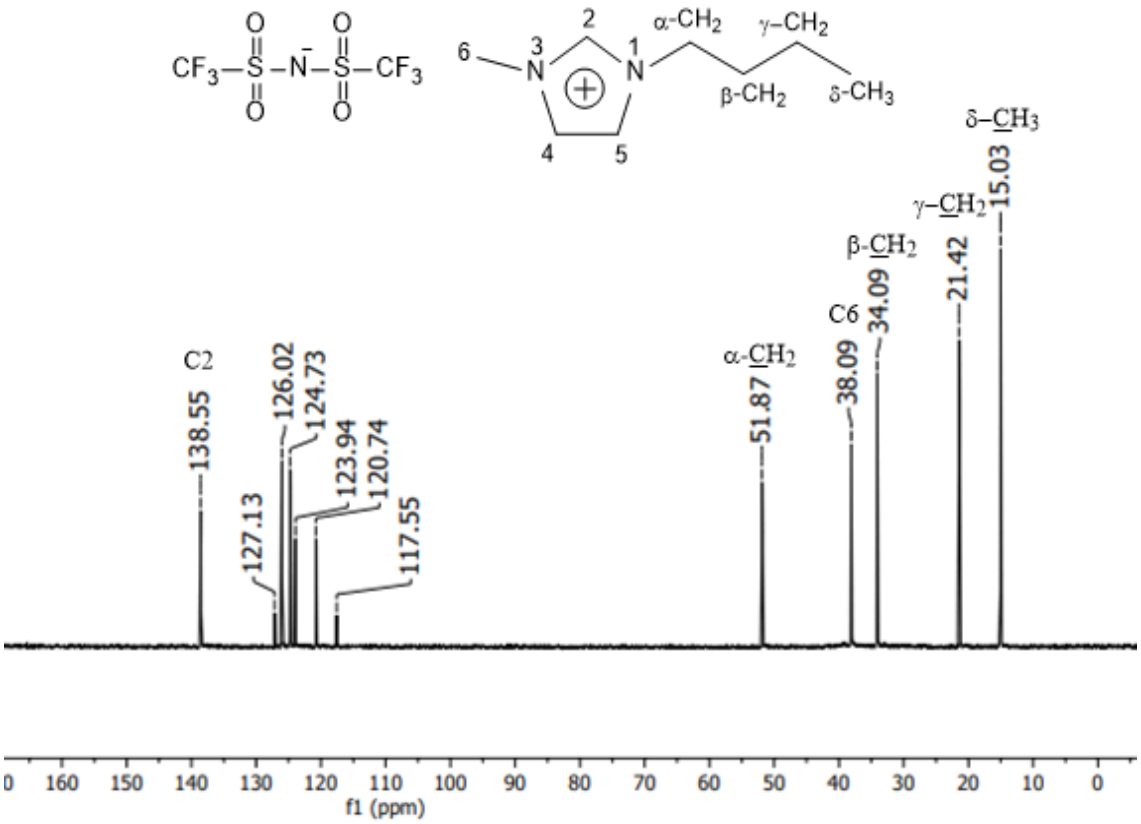

Figure S3. ^{13}C NMR spectrum (100.51 MHz) of Ionic Liquid [BMIM·NTf_2^-] at 298K.

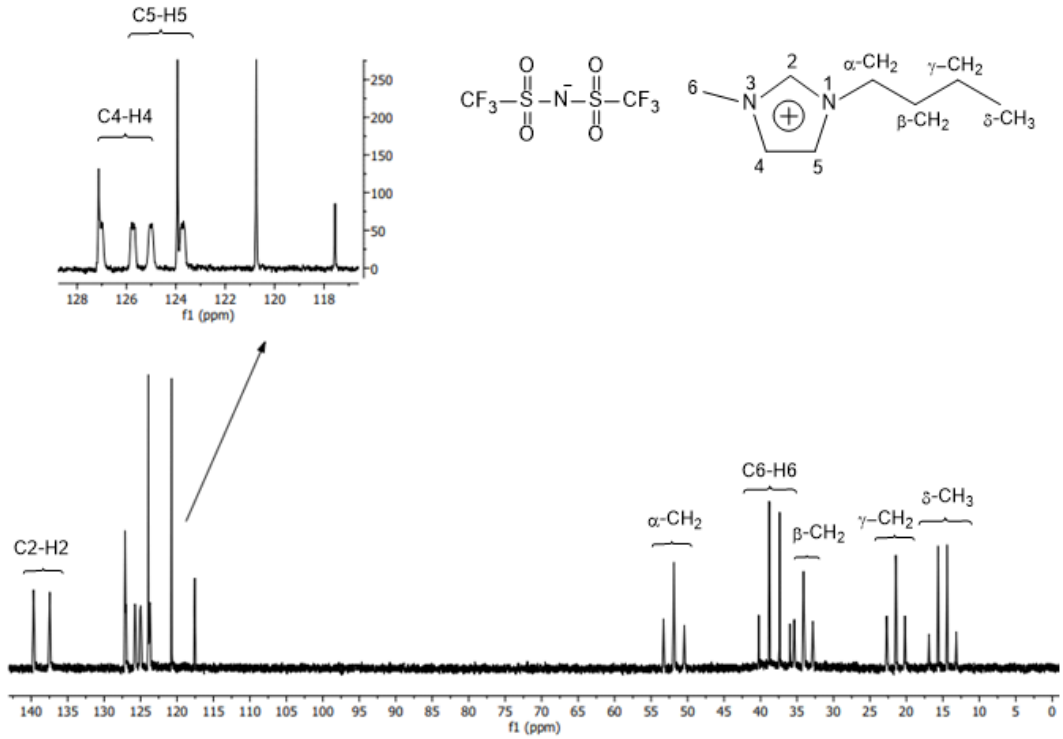

Figure S4. $\{^{1}H\}$-^{13}Cgated-decoupled spectrum of [BMIM·NTf_2^-] on DMA/ ACN gel (75:25 v/v) in the relaxed state.

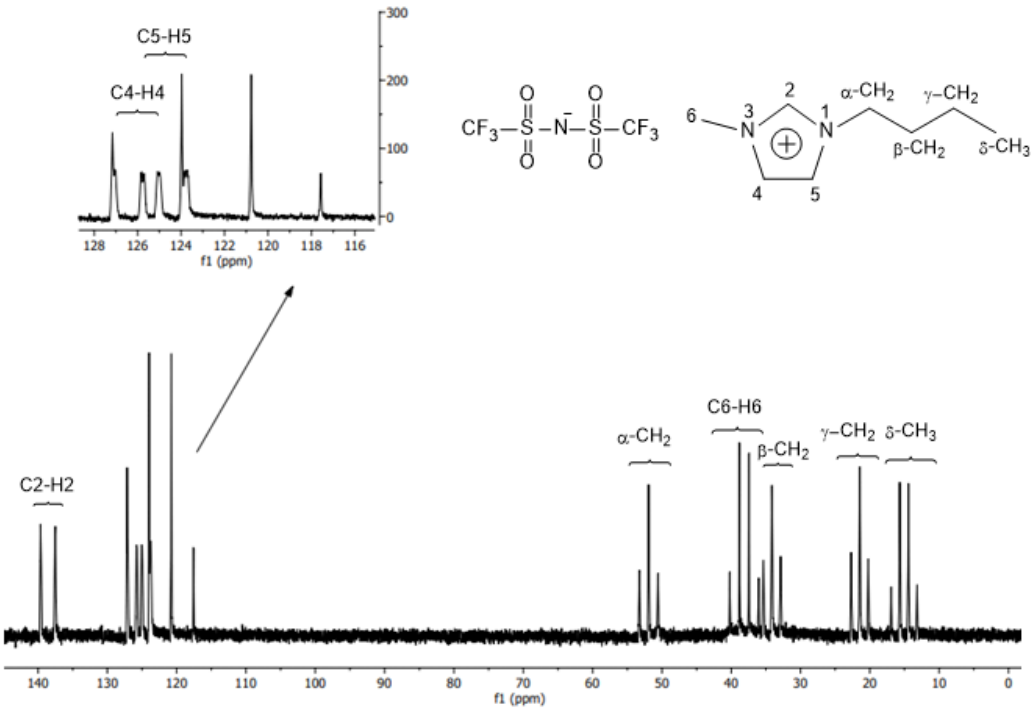

Figure S5. $\{^{1}H\}$-^{13}C gated-coupled spectrum of [BMIM·NTf_2^-] on DMAC/ ACN gel (75:25 v/v) in the compressed state.

3. NMR spectra of Ionic Liquid EMIM·BF_4^-

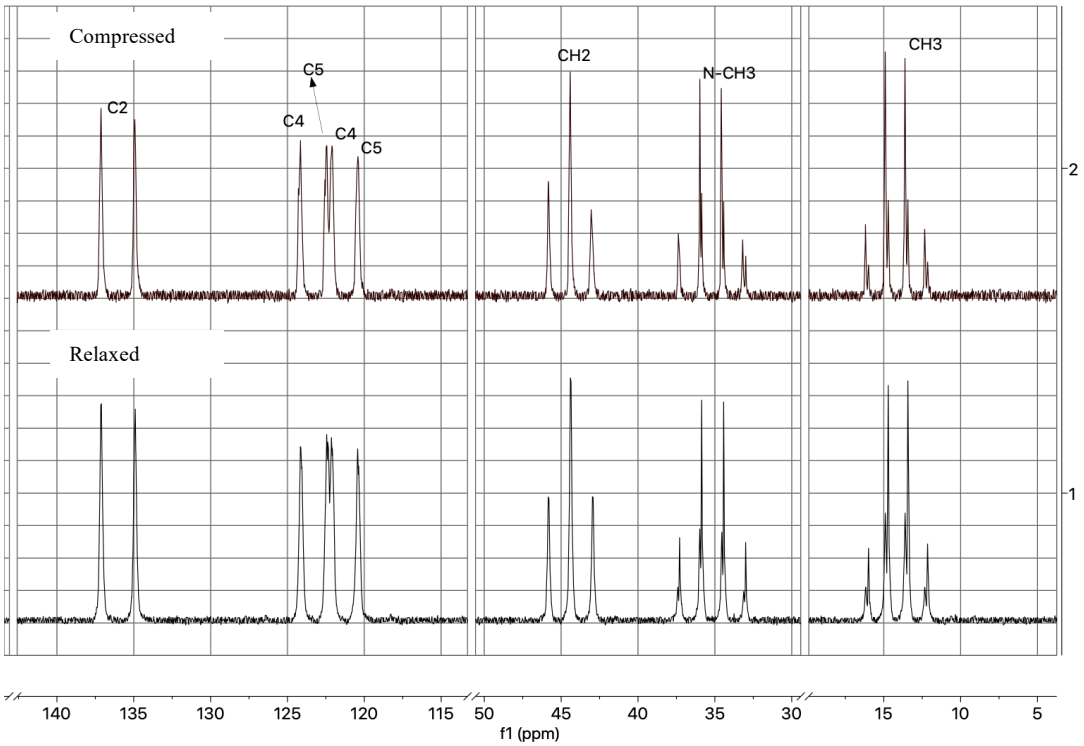

Figure S6. {^{1}H}-^{13}C-gated-decoupled spectra for the compressed and relaxed EMIM·BF_4^- /(DMA/ACN 75:25) system.

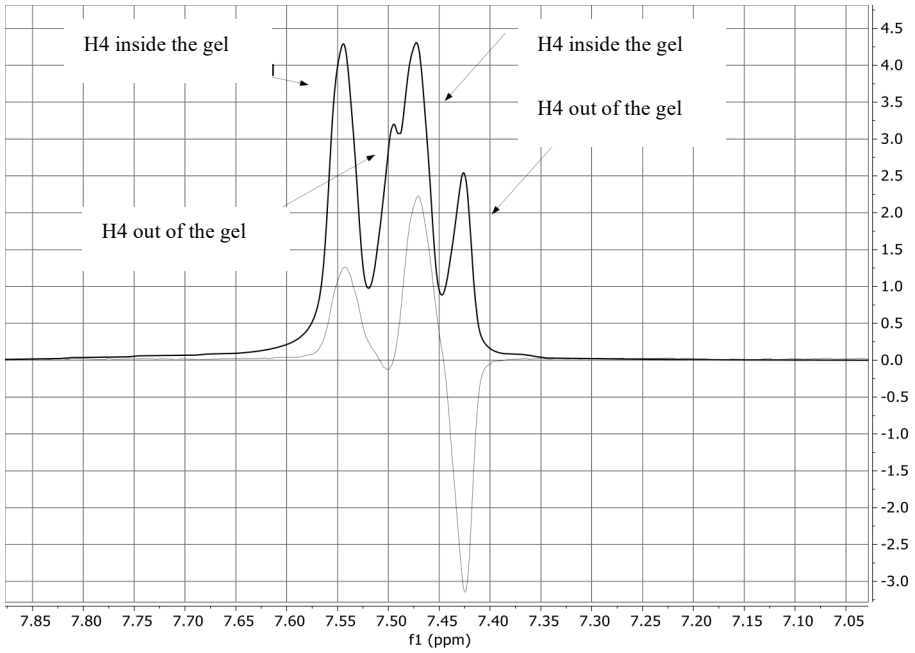

Figure S7. Red: ^{1}H spectrum; blue: H4 region in the 1D-NOESY spectrum of EMIM·BF_4^- (mixing time=500 ms) upon inversion of the methyl signal at position 6. Note the different sign of the NOE effect for the isotropic IL vs the IL inside the gel.

4. NMR spectra of Ionic Liquid BMIM·$[N(CN)_2]^-$

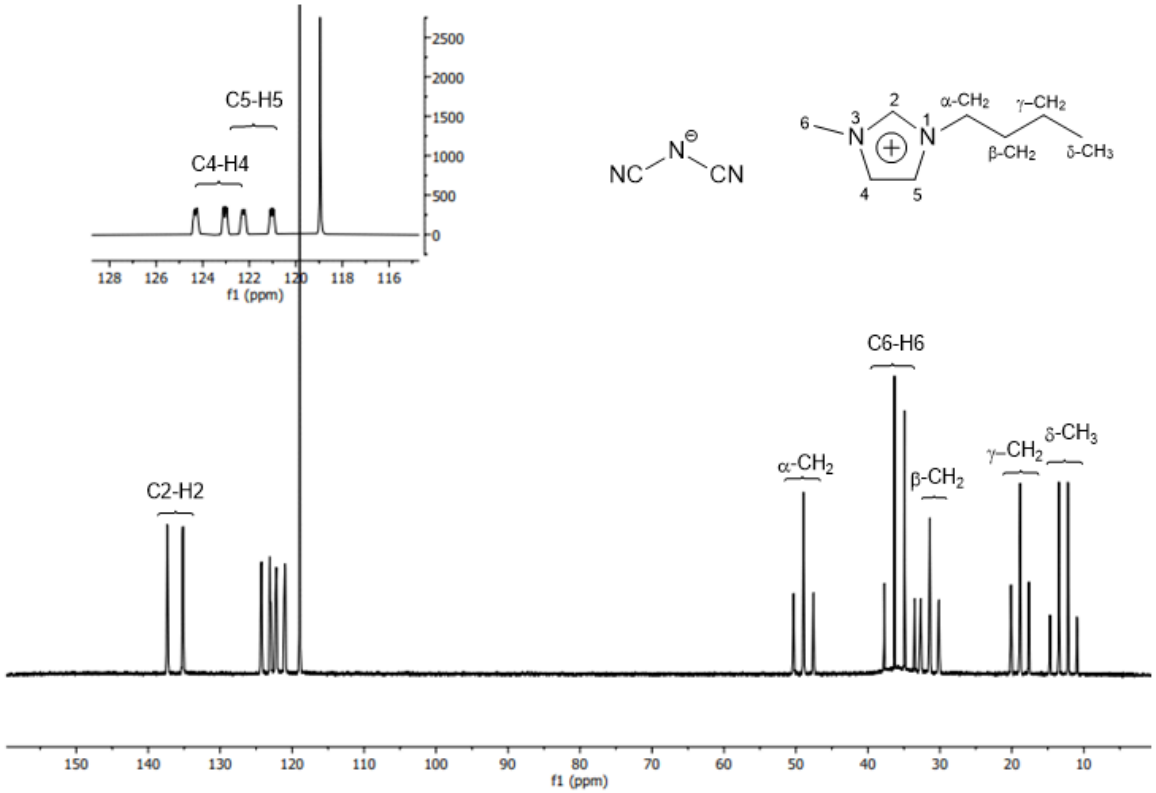

Figure S8. {^{1}H}-^{13}C gated-decoupled spectrum of BMIM. $[N(CN)_2]^-$ on DMA/ ACN gel (75:25 v/v) in compressed state.

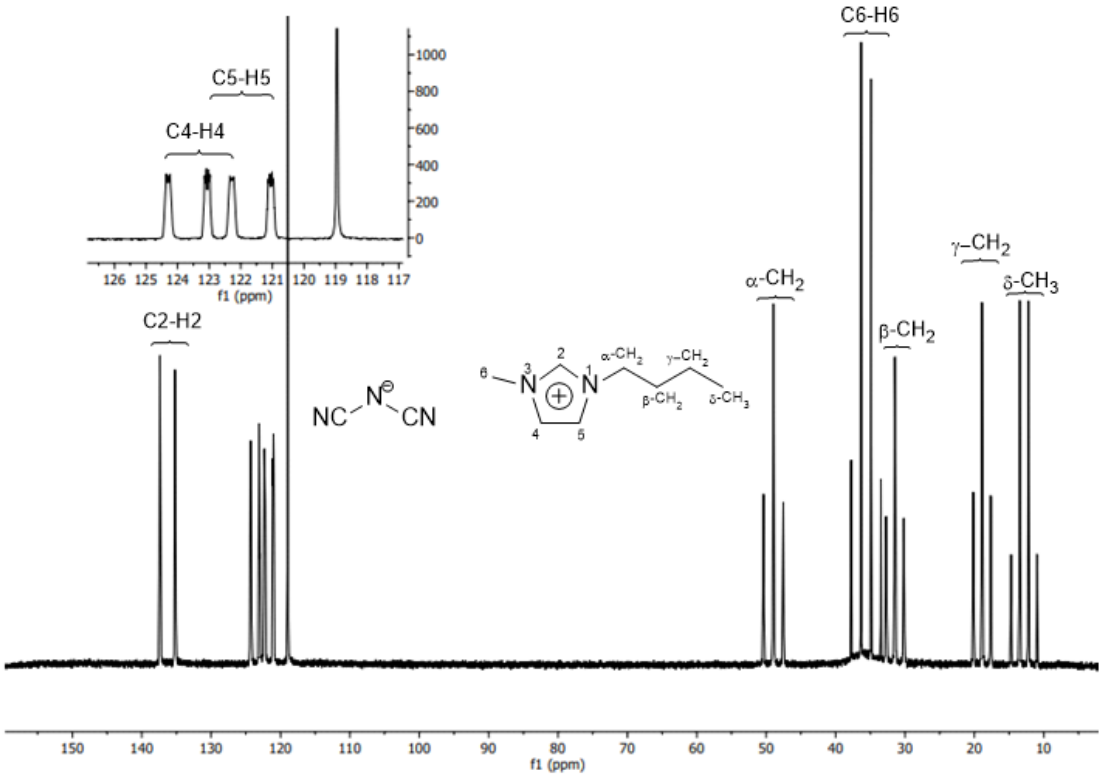

Figure S19. $\{^{1}H\}$-^{13}C gated-decoupled spectrum of BMIM·$[N(CN)_2]^-$ on DMA/ACN gel (75:25 v/v) in relaxed state.

5. RDC based conformational analysis of BMIM cation (BMIM·NTf_2^-)

The conformational space of the BMIM cation was first explored using the GMMX program inside the MNova/StereoFitter 14.2 package[2] and the MMFF94 force field. All enantiomeric conformations are discarded by the GMMX program. The nine obtained conformations were optimized at the M062X/6-31+G** level of theory using the Gaussian09[3] package and the ultrafine grid.

The $^{1}D^{CH}$ obtained RDCs were then fit to each of the obtained geometries using the Singular Value Decomposition procedure as implemented in the MSpin package.[4] The quality of the fitting is expressed in terms of the quality factor (Table S1).[5]

$$Q = \sqrt{\frac{\sum_i \left(D_i^{exp} - D_i^{calc}\right)^2}{\sum_i \left(D_i^{exp}\right)^2}}$$

A single tensor multi-conformer analysis of the BMIM cation was performed in the following way. First all conformations were aligned by minimizing the least-square distance between heavy atoms

in the molecule using mass weighted coordinates. Since only eight $^1D_{CH}$ RDCs were measured it is not possible to determine the populations for the nine conformations. Hence, all possible combinations of conformations, with increasing number of conformers, were generated and populations fit, using the MNova/StereoFitter software, using a described procedure where alignment tensor components and populations are simultaneously fit (Table S2). [6]

Table S1. Conformations found for the BMIM cation from the adjustment of the RDC for each structure individually

Conformation	Type	ΔE (kcal/mol)	*Q*
#1	G+A	0.00	0.217
#2	G-A	0.47	0.204
#3	AA	0.70	0.199
#4	G+G+	0.14	0.136
#5	G-G-	0.64	0.293
#6	AG+	1.11	0.234
#7	AG-	1.08	0.303
#8	G+G-	1.02	0.213
#9	G-G+	1.44	0.329

a) SCF M062X/6-31+G** energy differences

Table S2. Set of conformations found from the *Q* factor.

Number conformations	Conformation	Population (%)	Q
1	G+G+	100	0.136
2	G+G+; G-G-	93, 7	0.083

There is an important decrease in the quality factor by allowing the G+G+ conformation to mix with the G-G-. However, examination of the individual contributions of the RDCs to the conformationally averaged RDCs shows very large RDCs for individual conformations. The large GDO[7] value of ($2.9 \bullet 10^{-3}$) that the good quality of the fitting could be probably artifactual and the single-tensor procedure is a too rough approximation for such a small system where conformational jumping largely modifies the overall molecular shape.

Coupling	Exp.	G+G+[a]	G-G-[a]	G+G+[b]	G-G-[b]	G+G+/G-G-[c]
δ-$\underline{CH_3}$	-0.1	1.8	3.7	-0.0	9.7	0.6
γ-$\underline{CH_2}$	-0.8	-0.9	0.4	-4.0	36.2	-1.3
β-$\underline{CH_2}$	-3.8	-4.1	-3.3	-2.4	-15.9	-3.3
α-$\underline{CH_2}$	-8.2	-8.3	-6.9	-6.3	-42.6	-8.7
6	-3.8	-4.2	-4.8	-3.8	-8.1	-4.1
5	-1.1	-1.2	-0.8	0.7	-31.0	-1.4
4	5.3	5.3	4.7	9.3	-55.5	4.9
2	-10.7	-10.0	-10.1	-4.0	-98.8	-10.4

a) Single conformer SVD fitting b) Predicted RDCs in single tensor fitting of a 93:7 G+G+/G-G- ensemble c) Predicted conformationally averaged RDCs in single tensor fitting of a 93:7 G+G+/G-G- ensemble

6. MDOC simulations

6.1 Parametrization of the MDOC simulations

We moved then to the MDOC procedure[8] where the $^1D_{CH}$ RDCs act as time-average constraints[9] over a force-field based molecular dynamics simulation. The COSMOS polarizable force-field.[10][11] was employed in the MD run as implemented in the COSMOS 6.0 software package.[12] Simulation of the BMIM system made used of the same RDC constraints as in the above single-tensor analysis. Two MDOC simulations are performed: MDOC 1 with only RDC constrains and in MDOC 2 constraints from $^3J_{HH}$ couplings are added. The parameters for the MDOC runs are given in Table 1.

Table 1: Simulation parameters for MDOC Simulations

General parameters for the MDOC simulation	
Parameter	Value
Target temperature	290 K
Mean temperature	303.5 K
MD time step	0.5 fs
Total MDOC duration	40 ns
BPT atomic charge calculation	2 fs
Coupling time η to the heat bath	0.02 ps
Memory decay time τ for running RDC average	200 ps
Time constant ρ for the exponential rise of pseudo-forces	200 ps
Order parameter of the alignment medium S_{am}	0.004
Width parameters for the RDC pseudo forces	0.5 Hz
Weight parameters for the RDC pseudo forces	0.0003 kJ mol^{-1} Hz^{-1}
Pseudo-force width ΔJ for the $^3J_{HH}$ coupling constraints	1.0 Hz
Weight parameter for the pseudo-forces of the $^3J_{HH}$ couplings	6 kJ mol^{-1} Hz^{-1}

6.2 MDOC Results

Table S3: Experimental RDC compared with calculated values from the MDOC simulation 1 with RDC constrains only on BMIM·NTf_2^-

Coupling proton	Coupling carbon	RDC exp. / Hz	RDC calc. / Hz	Diff. / Hz	Error exp. / Hz
H5	C5	-1.1	-1.3014	0.201	0.5
H4	C4	5.3	5.0259	0.274	0.5
H2	C2	-10.7	-10.3465	-0.353	0.5
H6c	C6	-3.8	-3.6184	-0.182	0.5
H6a	C6	-3.8	-3.6146	-0.185	0.5
H6b	C6	-3.8	-3.6200	-0.180	0.5
Ha_proS	Ca	-8.2	-8.0180	-0.182	0.5
Ha_proR	Ca	-8.2	-8.0135	-0.186	0.5
Hb_proS	Cb	-3.8	-3.7379	-0.062	0.5
Hb_proR	Cb	-3.8	-3.7316	-0.068	0.5
Hg_proS	Cg	-0.8	-0.8347	0.035	0.5
Hg_proR	Cg	-0.8	-0.8331	0.033	0.5
Hdb	Cd	-0.1	-0.0616	-0.038	0.5
Hda	Cd	-0.1	-0.0590	-0.041	0.5
Hdc	Cd	-0.1	-0.0645	-0.036	0.5

Quality n/χ^2 = 8.85

Table S4: Experimental RDC compared with calculated values from the MDOC simulation 2 with RDC and $^3J_{HH}$ constraints on BMIM·NTf_2^-

Coupling proton	Coupling carbon	RDC exp. / Hz	RDC calc. / Hz	Diff. / Hz	Error exp. / Hz
H5	C5	-1.1	-1.2965	0.196	0.5
H4	C4	5.3	5.0440	0.256	0.5
H2	C2	-10.7	-10.360	-0.340	0.5
H6c	C6	-3.8	-3.6365	-0.164	0.5
H6a	C6	-3.8	-3.6342	-0.166	0.5
H6b	C6	-3.8	-3.6336	-0.166	0.5
Ha_proS	Ca	-8.2	-8.0309	-0.169	0.5
Ha_proR	Ca	-8.2	-8.0269	-0.173	0.5
Hb_proS	Cb	-3.8	-3.7796	-0.020	0.5
Hb_proR	Cb	-3.8	-3.7345	-0.066	0.5
Hg_proS	Cg	-0.8	-0.8617	0.062	0.5
Hg_proR	Cg	-0.8	-0.8491	0.049	0.5
Hdb	Cd	-0.1	-0.0577	-0.042	0.5
Hda	Cd	-0.1	-0.0617	-0.038	0.5
Hdc	Cd	-0.1	-0.0482	-0.052	0.5

Quality n/χ^2 = 9.95

Table S5: Experimental $^3J_{HH}$ compared with calculated values from the MDOC simulation 2 with RDC and $^3J_{HH}$ constraints on BMIM·NTf_2^-

Atom A	Atom B	$^3J_{HH}$ Exp. /Hz	$^3J_{HH}$ Calc. MDOC Sim. /Hz	$^3J_{HH}$ Calc. Start Molecule /Hz	Diff MDOC Sim. – Exp, /Hz	Error Exp.+ Calc. /Hz
Ha_proS	Hb_proS	7.2	6.825	4.133	-0.375	1.15
Ha_proS	Hb_proR	7.2	6.335	3.549	-0.865	1.15
Ha_proR	Hb_proS	7.2	6.564	12.671	-0.636	1.15
Ha_proR	Hb_proR	7.2	6.688	2.388	-0.512	1.15
Hb_proS	Hg_proS	7.2	6.887	13.282	-0.313	1.15
Hb_proS	Hg_proR	7.2	6.536	3.162	-0.664	1.15
Hb_proR	Hg_proS	7.2	6.726	1.933	-0.474	1.15
Hb_proR	Hg_proR	7.2	6.868	13.282	-0.332	1.15
Hg_proS	Hdb	7.2	6.836	2.975	-0.364	1.15
Hg_proS	Hda	7.2	6.839	3.320	-0.361	1.15
Hg_proS	Hdc	7.2	6.837	13.994	-0.363	1.15
Hg_proR	Hdb	7.2	6.783	13.988	-0.417	1.15
Hg_proR	Hda	7.2	6.782	3.383	-0.418	1.15
Hg_proR	Hdc	7.2	6.786	2.534	-0.414	1.15

Quality n/χ^2 = 5.54

6.3 Comparison of the MDOC simulation with only RDC constraints (MDOC 1) and the simulation including $^3J_{HH}$ constraints (MDOC 2)

Both simulations MDOC 1 and 2 are performed with the same simulation parameters – the only difference in MDOC 2 was that the pseudo-forces for the $^3J_{HH}$ couplings are introduced. The calculation of the $^3J_{HH}$ couplings was performed using the Altona equation (for details see [13]). Comparing the RDC tables S3 and S4 the additional constraints support the RDC results and lead to a slightly better score. As displayed in Fig S20 the case of the (N1-**Ca-Cb**-Cg) dihedral the population of the G- is suppressed and that of the G+ and A states got larger. The same holds partly for the (Ca-**Cb-Cg**-Cd) torsion.

An analysis of the combination of the torsions around Ca-Cb and Cb-Cg is given in table S4. Obviously, the action of the $^3J_{HH}$ constraints has a marked influence on distribution of conformers.

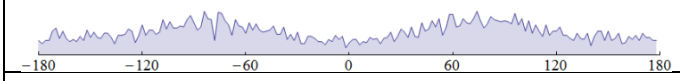	(C2-**N1-Cα**-Cβ) Rotation about the N1-Cα bond Slight preference of C_β perpendicular to the ring plane **MDOC 1**
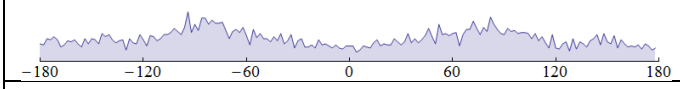	(C2-**N1-Cα**-Cβ) MDOC 2
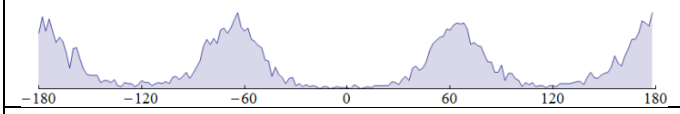	(N1-**Cα-Cβ**-Cγ) Rotation about the Cα-Cβ bond Ranges {Anti, Gauge -, Gauge +} Ratio: {0.368, 0.324, 0.308} **MDOC 1**
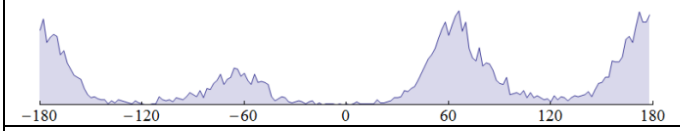	(N1-**Cα-Cβ**-Cγ) Ratio: {0.44, 0.159, 0.401} MDOC 2
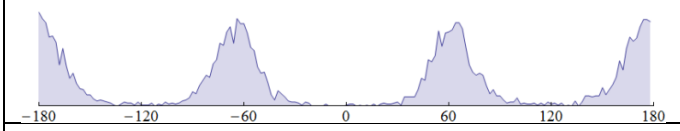	(Cα-**Cβ-Cγ**-Cδ) Rotation about the **Cβ-Cγ** bond Ranges: {Anti, Gauge -, Gauge +} Ratio: {0.398, 0.305, 0.297} MDOC 1
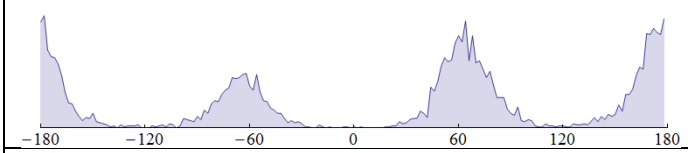	(Cα-**Cβ-Cγ**-Cδ) Ratio: {0.418, 0.211, 0.371} MDOC 2
Figure S20 Torsion distributions from the MDOC 1 and MDOC 2 simulations on BMIM·NTf_2^-	Remarks

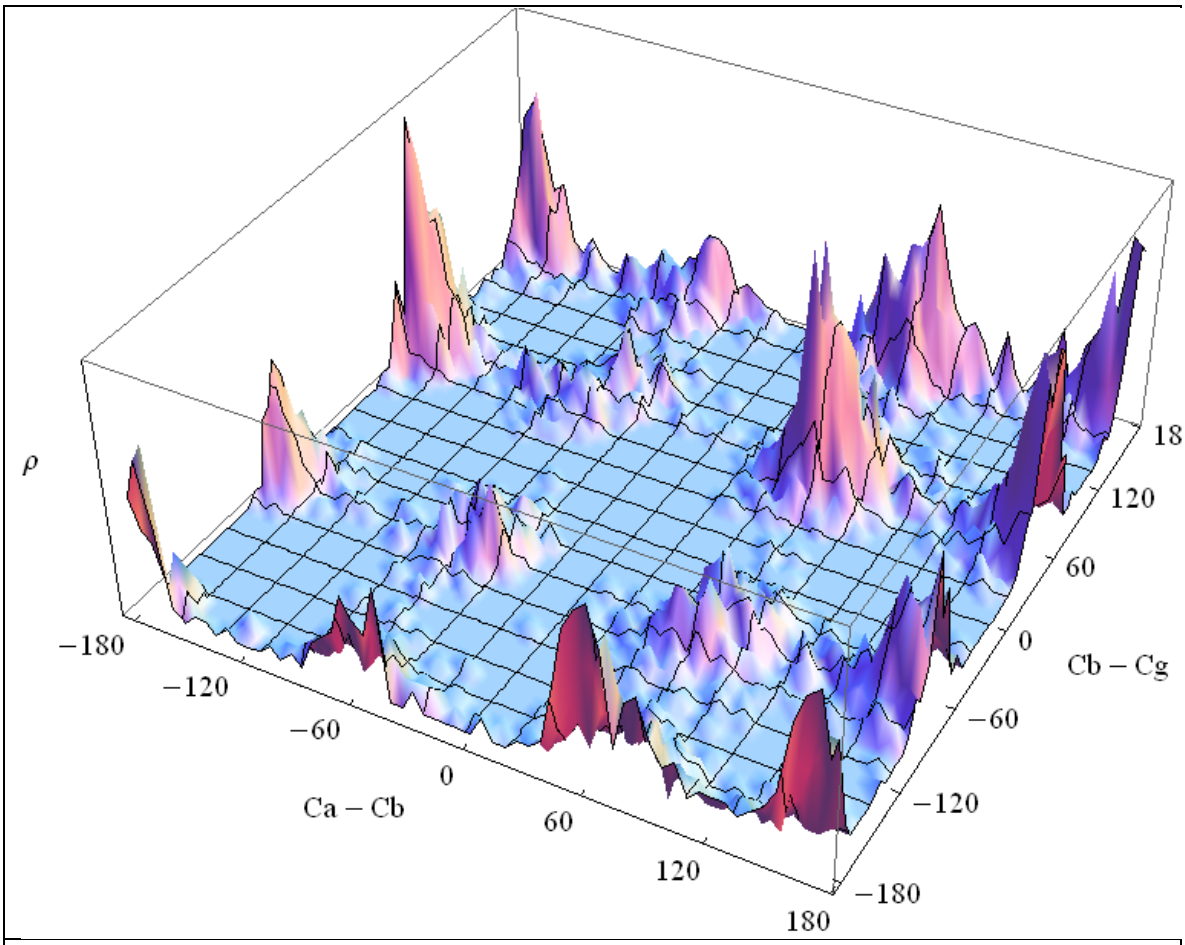

Figure S21: 2D map of conformer populations for the internal coordinates {N1-**Cα-Cβ**-Cγ} (Ca-Cb) and {Cα-**Cβ-Cγ**-Cδ} (Cb-Cg) for the MDOC 2 simulation with RDC and $^3J_{HH}$ constraints. The combinations {G-, G+}, {G+, G-} and {G-, G-} are less populated (the full population analysis is given in table S4)

Table S4: Conformer statistics for the torsion {N1-**Cα-Cβ**-Cγ} and {Cα-**Cβ-Cγ**-Cδ}

Conformer	Population / % RDC constraints only	Population / % RDC and $^3J_{HH}$ constraints	Remarks
G+A	14.7	18.3	The following ranges are assumed:
G-A	15.1	7.5	Anti {-180 to -120 and 120 to 180}
AA	10.0	16.0	Gauge + {0 to 120}
G+G+	10.2	15.2	Gauge - {-120 to 0}
G-G-	10.8	4.1	
AG+	13.0	17.6	
AG-	13.8	10.4	
G+G-	5.9	6.7	
G-G+	6.6	4.3	

7. Swelling of cross-linked DMA/ACN gels in different ionic liquids

Sticks between 1-2 cm of the 0.5% cross-linked DMAC/ACN copolymer gel (0.0425 mmol EGDA) were cut and allowed to swell in BMIM·NTf_2^-, BMIM·BF_4^-, BMIM·PF_6^-, EMIM·BF_4^- and BMIM·$[N(CN)_2]^-$. The sticks swelled, at room temperature, in all ionic liquids except BMIM·PF_6^-. Furthermore, we found that in some ionic liquids the swelling process was faster, for example, the DMA/ACN copolymer gel takes a week to swell in BMIM.$[N(CN)_2]^-$, while in BMIM·NTf_2^- and EMIM·BF_4^- takes about a month. The swollen sticks grew to twice their original size.

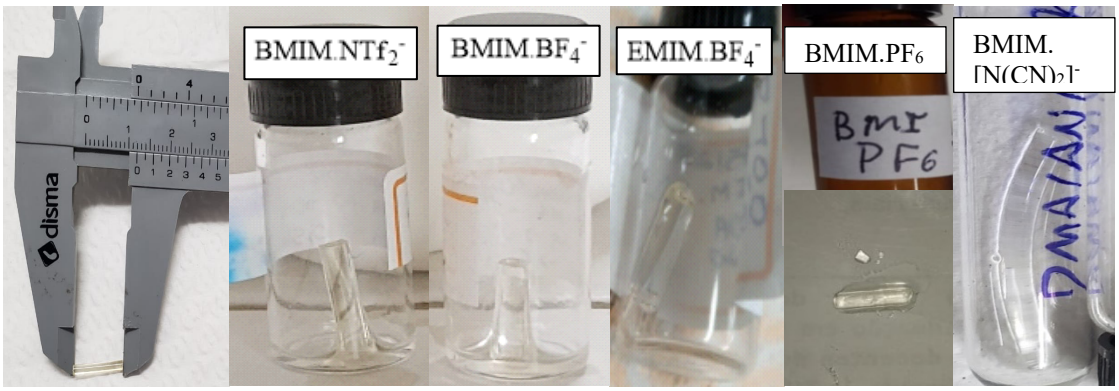

Figure S10. Swelling of DMAC/ACN gels in different ionic liquids.

8. BMIM cation XYZ geometries (Å)

```
25
#1 E(RM062X) =  -422.995906239 G+A
C     -0.442000   -0.755900    0.767200
C      0.696100   -0.026300    0.934400
N      0.855100    0.736400   -0.201300
C     -0.156000    0.476000   -1.031800
N     -0.953200   -0.430000   -0.468600
C      1.959000    1.667900   -0.455000
C     -2.225400   -0.928100   -1.028800
C     -3.424600   -0.351700   -0.281400
C     -3.483700    1.174800   -0.307400
C     -4.752800    1.709000    0.354300
```

```
H     -0.921000   -1.475400    1.413200
H      1.400800    0.010600    1.750800
H     -0.305700    0.927300   -2.002000
H      1.972200    2.428800    0.325300
H      1.802400    2.140900   -1.423300
H      2.899800    1.117500   -0.464300
H     -2.193300   -2.018700   -0.979500
H     -2.237600   -0.634300   -2.081500
H     -3.422800   -0.712000    0.755000
H     -4.322300   -0.769700   -0.750700
H     -3.435500    1.522300   -1.348400
H     -2.605800    1.588600    0.207400
H     -5.645300    1.345700   -0.162800
H     -4.776000    2.800500    0.337300
H     -4.814500    1.387800    1.398300

25
#2 E(RM062X) =  -422.995150721 G-A
C     -0.441700   -0.756100    0.766600
C      0.696300   -0.026000    0.934800
N      0.854800    0.736200   -0.201100
C     -0.155500    0.475900   -1.032200
N     -0.954000   -0.430000   -0.468200
C      1.963000    1.662000   -0.457400
C     -2.219400   -0.930600   -1.045800
C     -3.373500    0.041300   -0.815800
C     -3.664300    0.320700    0.658300
C     -4.894100    1.209200    0.836800
H     -0.925200   -1.472100    1.413000
H      1.399100    0.013400    1.752500
H     -0.299000    0.921500   -2.006000
H      2.900700    1.106400   -0.469000
H      1.806700    2.136300   -1.425100
H      1.982000    2.422200    0.323300
H     -2.040700   -1.109800   -2.108200
H     -2.409500   -1.894900   -0.568700
H     -3.172500    0.981300   -1.345800
```

```
H     -4.257000   -0.398800   -1.292200
H     -3.816800   -0.631200    1.184200
H     -2.796100    0.804700    1.124600
H     -5.784800    0.732200    0.418400
H     -5.085000    1.408300    1.893200
H     -4.759300    2.170900    0.332800

25
#3 E(RM062X) =  -422.994791124 AA
C     -0.441500   -0.756300    0.767100
C      0.696100   -0.026300    0.934600
N      0.854800    0.736600   -0.201100
C     -0.155400    0.475500   -1.032200
N     -0.953900   -0.429500   -0.468400
C      1.957600    1.669900   -0.453400
C     -2.212600   -0.947700   -1.039700
C     -3.436800   -0.346400   -0.357600
C     -4.731400   -0.889000   -0.965600
C     -5.967300   -0.298500   -0.290200
H     -0.920900   -1.476100    1.412500
H      1.399600    0.012300    1.751700
H     -0.300800    0.922400   -2.004900
H      2.900000    1.122000   -0.451800
H      1.807000    2.135300   -1.426300
H      1.963000    2.436400    0.321400
H     -2.196800   -0.712900   -2.107100
H     -2.187300   -2.035600   -0.935500
H     -3.408900   -0.574300    0.715300
H     -3.405100    0.746000   -0.454900
H     -4.751900   -0.662600   -2.038700
H     -4.745900   -1.981900   -0.874700
H     -5.988800    0.790500   -0.393100
H     -6.881800   -0.694800   -0.735700
H     -5.983700   -0.538000    0.777200

25
#4 E(RM062X) =  -422.995682240 G+G+
```

```
C     -0.441800   -0.756000    0.767100
C      0.696100   -0.026200    0.934500
N      0.855200    0.736400   -0.201200
C     -0.156000    0.475800   -1.031800
N     -0.953600   -0.429900   -0.468700
C      1.958000    1.669200   -0.454000
C     -2.220200   -0.938800   -1.032200
C     -3.419900   -0.433100   -0.233100
C     -3.510100    1.092100   -0.143300
C     -3.649200    1.781100   -1.500600
H     -0.920000   -1.475500    1.413500
H      1.400000    0.011600    1.751500
H     -0.301500    0.923700   -2.004000
H      1.806400    2.135400   -1.426400
H      2.900100    1.120900   -0.454200
H      1.964900    2.435000    0.321400
H     -2.160800   -2.029300   -1.028100
H     -2.255200   -0.606500   -2.071800
H     -3.393300   -0.869700    0.771700
H     -4.315400   -0.834300   -0.720800
H     -2.635700    1.485100    0.393900
H     -4.375000    1.341300    0.478200
H     -2.759300    1.657600   -2.128600
H     -3.806400    2.854800   -1.378200
H     -4.501700    1.381300   -2.058300

25
#5 E(RM062X) =  -422.994887463 G-G-
C     -0.441700   -0.756000    0.766500
C      0.696400   -0.025800    0.934800
N      0.855000    0.736000   -0.201000
C     -0.155500    0.476000   -1.031900
N     -0.954200   -0.430300   -0.468300
C      1.962700    1.662300   -0.457300
C     -2.219400   -0.928200   -1.048400
C     -3.352800    0.081500   -0.873400
C     -3.659000    0.439100    0.583100
```

```
C     -4.139100   -0.747300    1.418800
H     -0.922200   -1.473900    1.412800
H      1.399100    0.013500    1.752500
H     -0.298900    0.922000   -2.005600
H      2.900500    1.106800   -0.470300
H      1.805500    2.137700   -1.424300
H      1.982200    2.421600    0.324300
H     -2.030400   -1.143200   -2.102400
H     -2.432500   -1.874800   -0.548400
H     -3.112500    0.987100   -1.443300
H     -4.240600   -0.355800   -1.344300
H     -2.776900    0.899400    1.048700
H     -4.431400    1.213900    0.582200
H     -3.373300   -1.522700    1.531100
H     -4.419000   -0.426200    2.424300
H     -5.016100   -1.217000    0.963100

25
#6 E(RM062X) =  -422.994137160 AG+
C     -0.441500   -0.756300    0.767000
C      0.696100   -0.026100    0.934600
N      0.854900    0.736400   -0.201100
C     -0.155600    0.475600   -1.032100
N     -0.953900   -0.429600   -0.468400
C      1.957100    1.670800   -0.452800
C     -2.212700   -0.947900   -1.038800
C     -3.432000   -0.327300   -0.361500
C     -4.741400   -0.794800   -1.005500
C     -4.970700   -2.303100   -0.907700
H     -0.920900   -1.476300    1.412200
H      1.399600    0.012200    1.751900
H     -0.300900    0.922500   -2.004800
H      2.900900    1.125800   -0.436800
H      1.814300    2.125200   -1.432100
H      1.952900    2.445500    0.313900
H     -2.195300   -0.721400   -2.108400
H     -2.186600   -2.033700   -0.924100
```

```
H     -3.429100   -0.593900    0.703000
H     -3.351600    0.764100   -0.422500
H     -5.562100   -0.268000   -0.510200
H     -4.763600   -0.478300   -2.055500
H     -4.893800   -2.646400    0.129600
H     -5.967800   -2.564600   -1.267800
H     -4.255500   -2.872900   -1.509300

25
#7 E(RM062X) =  -422.994189575 AG-
C     -0.441500   -0.756200    0.767100
C      0.696100   -0.026400    0.934600
N      0.854800    0.736800   -0.201100
C     -0.155400    0.475400   -1.032200
N     -0.954000   -0.429500   -0.468400
C      1.957400    1.670300   -0.453200
C     -2.211200   -0.948400   -1.041800
C     -3.433000   -0.339700   -0.358600
C     -4.739900   -0.932400   -0.895500
C     -4.960600   -0.682800   -2.387600
H     -0.920400   -1.476500    1.412300
H      1.399800    0.011800    1.751700
H     -0.301100    0.922500   -2.004800
H      1.962300    2.436900    0.321600
H      1.806800    2.135600   -1.426100
H      2.899800    1.122600   -0.451400
H     -2.189800   -2.036400   -0.931000
H     -2.186500   -0.718500   -2.109000
H     -3.422700    0.746500   -0.513300
H     -3.363700   -0.513600    0.721300
H     -5.563500   -0.491800   -0.326200
H     -4.764100   -2.008900   -0.687100
H     -4.880600    0.383700   -2.624200
H     -5.956500   -1.013200   -2.689600
H     -4.243200   -1.226200   -3.010900

25
```

#8 E(RM062X) = -422.994276346 G+G-

C	-0.441900	-0.756400	0.766800
C	0.696000	-0.026300	0.934500
N	0.854800	0.736700	-0.201200
C	-0.155700	0.475400	-1.032300
N	-0.953200	-0.429400	-0.467800
C	1.960200	1.666300	-0.455400
C	-2.236400	-0.907000	-1.017700
C	-3.436800	-0.298100	-0.296300
C	-3.502700	1.235400	-0.343000
C	-2.731400	1.946700	0.772800
H	-0.923900	-1.472100	1.414900
H	1.400600	0.010900	1.750900
H	-0.304800	0.926700	-2.002500
H	2.899400	1.113600	-0.472000
H	1.800000	2.145100	-1.420300
H	1.978700	2.422800	0.328900
H	-2.239000	-0.636900	-2.076800
H	-2.229200	-1.996900	-0.945800
H	-4.319800	-0.728200	-0.780000
H	-3.458100	-0.645600	0.744000
H	-3.164100	1.588400	-1.327300
H	-4.552700	1.532400	-0.271400
H	-1.650200	1.775400	0.728800
H	-2.890700	3.026200	0.720600
H	-3.077600	1.609500	1.754700

25

#9 E(RM062X) = -422.993604124 G-G+

C	-0.441800	-0.756200	0.765900
C	0.696500	-0.025700	0.935000
N	0.854500	0.735900	-0.201000
C	-0.155400	0.475700	-1.032300
N	-0.953800	-0.429700	-0.467600
C	1.960000	1.665400	-0.455500
C	-2.234000	-0.906200	-1.031000
C	-3.313700	0.173500	-1.021800

C	-3.621100	0.770300	0.359400
C	-2.718100	1.937100	0.771300
H	-0.924500	-1.471800	1.413300
H	1.399600	0.013400	1.752400
H	-0.302800	0.928400	-2.002300
H	2.899200	1.112400	-0.470400
H	1.800600	2.143100	-1.421000
H	1.977500	2.422500	0.328300
H	-2.033400	-1.270900	-2.041200
H	-2.529300	-1.760100	-0.417400
H	-3.043800	0.972400	-1.724500
H	-4.209400	-0.302500	-1.434100
H	-4.654300	1.128300	0.349200
H	-3.588900	-0.022200	1.119300
H	-2.737100	2.725200	0.011400
H	-3.066300	2.377100	1.708500
H	-1.675800	1.639100	0.928200

9. References

[1] K. Stott, J. Keeler, Q. N. Van, A. J. Shaka, *J. Magn. Reson.* **1997**, *125*, 302–324.

[2] MNova 14.1 https://mestrelab.com/software/mnova/, **2022.**

[3] Gaussian 09, Revision C.01, M. J. Frisch, G. W. Trucks, H. B. Schlegel, G. E. Scuseria, M. A. Robb, J. R. Cheeseman, G. Scalmani, V. Barone, G. A. Petersson, H. Nakatsuji, X. Li, M. Caricato, A. Marenich, J. Bloino, B. G. Janesko, R. Gomperts, B. Mennucci, H. P. Hratchian, J. V. Ortiz, A. F. Izmaylov, J. L. Sonnenberg, D. Williams-Young, F. Ding, F. Lipparini, F. Egidi, J. Goings, B. Peng, A. Petrone, T. Henderson, D. Ranasinghe, V. G. Zakrzewski, J. Gao, N. Rega, G. Zheng, W. Liang, M. Hada, M. Ehara, K. Toyota, R. Fukuda, J. Hasegawa, M. Ishida, T. Nakajima, Y. Honda, O. Kitao, H. Nakai, T. Vreven, K. Throssell, J. A. Montgomery, Jr., J. E. Peralta, F. Ogliaro, M. Bearpark, J. J. Heyd, E. Brothers, K. N. Kudin, V. N. Staroverov, T. Keith, R. Kobayashi, J. Normand, K. Raghavachari, A. Rendell, J. C. Burant, S. S. Iyengar, J. Tomasi, M. Cossi, J. M. Millam, M. Klene, C. Adamo, R. Cammi, J. W. Ochterski, R. L. Martin, K. Morokuma, O. Farkas, J. B. Foresman, and D. J. Fox, Gaussian, Inc., Wallingford CT, 2016**.**

[4] A. Navarro-Vázquez, *Magn. Reson. Chem.* **2012**, *50*, S73–S79.

[5] G. Cornilescu, J. L. Marquardt, M. Ottiger, A. Bax, *J. Am. Chem. Soc.* **1998**, *120*, 6836–6837.

[6] V. M. Sánchez-Pedregal, R. Santamaría-Fernández, A. Navarro-Vázquez, *Org. Lett.* **2009**, *11*, 1471–1474.

[7] F. Kramer, M. V. Deshmukh, H. Kessler, S. J. Glaser, *Concepts Magn. Reson. Part A* **2004**, *21A*, 10–21.

[8] P. Tzvetkova, U. Sternberg, T. Gloge, A. Navarro-Vázquez, B. Luy, *Chem. Sci.* **2019**, *10*, 8774–8791.

[9] A. E. Torda, R. M. Scheek, W. F. van Gunsteren, *Chem. Phys. Lett.* **1989**, *157*, 289–294.
[10] M. Möllhoff, U. Sternberg, *J. Mol. Model.* **2001**, *7*, 90–102.
[11] U. Sternberg, F.-T. Koch, M. Bräuer, M. Kunert, E. Anders, *J. Mol. Model.* **2001**, *7*, 54–64.
[12] COSMOS 6.0 http://www.cosmos-software.de/intro_e.html, **2022.**
[13] U. Sternberg, P. Tzvetkova, and C. Muhle-Goll, The Simulation of NMR Data of Flexible Molecules - Sagittamide A as Example for MD Simulations with Orientational Constraints; Phys. Chem. Chem. Phys., 2020, **22**, 17375, DOI: 10.1039/D0CP01905D.